ACS APPLIED MATERIALS & INTERFACES

Research Article

www.acsami.org

Rough Electrode Creates Excess Capacitance in Thin-Film Capacitors

Solmaz Torabi,*[,†] Megan Cherry,[†] Elisabeth A. Duijnstee,[†] Vincent M. Le Corre,[†] Li Qiu,[†,‡] Jan C. Hummelen,[†,‡] George Palasantzas,[†] and L. Jan Anton Koster[†]

[†]Zernike Institute for Advanced Materials, Nijenborgh 4, 9747 AG Groningen, The Netherlands

[‡]Stratingh Institute for Chemistry, Nijenborgh 4, 9747 AG Groningen, The Netherlands

Supporting Information

ABSTRACT: The parallel-plate capacitor equation is widely used in contemporary material research for nanoscale applications and nanoelectronics. To apply this equation, flat and smooth electrodes are assumed for a capacitor. This essential assumption is often violated for thin-film capacitors because the formation of nanoscale roughness at the electrode interface is very probable for thin films grown via common deposition methods. In this work, we experimentally and theoretically show that the electrical capacitance of thin-film capacitors with realistic interface roughness is significantly larger than the value predicted by the parallel-plate capacitor equation. The degree of the deviation depends on the strength of the roughness, which is described by three roughness parameters for a self-affine fractal surface. By applying an extended parallel-plate capacitor equation that includes the roughness parameters of the electrode, we are able to calculate the excess capacitance of the electrode with weak roughness. Moreover, we introduce the roughness parameter limits for which the simple parallel-plate capacitor equation is sufficiently accurate for capacitors with one rough electrode. Our results imply that the interface roughness beyond the proposed limits cannot be dismissed unless the independence of the capacitance from the interface roughness is experimentally demonstrated. The practical protocols suggested in our work for the reliable use of the parallel-plate capacitor equation can be applied as general guidelines in various fields of interest.

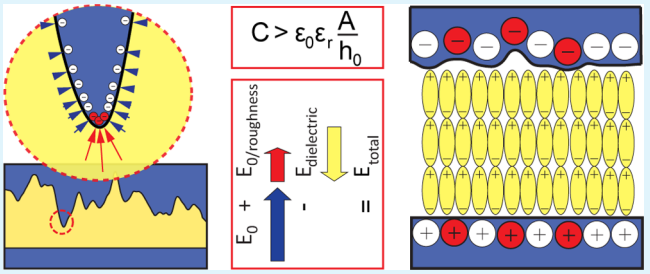

KEYWORDS: *parallel-plate capacitor equation, interface roughness, dielectric constant, capacitance, thin-film capacitors*

1. INTRODUCTION

The parallel-plate capacitor equation is one of the most basic equations in electrostatics. The equation states that the electrical capacitance (C) is linearly proportional to the area of the plates (A) and the relative dielectric constant of the filler material (ε_r) and inversely proportional to the spacing between the plates (h_0). This textbook formula is widely used in contemporary material research and electrical engineering for nanoscale applications. For instance, the determination of the electrical capacitance and the dielectric constant of a material is a crucial characterization step for the development of memories,[1,2] energy-storage devices,[3,4] embedded capacitors,[5,6] electroluminescent devices,[7] organic solar cells,[8,9] artificial muscles,[10,11] actuators,[12] smart skins,[13−15] and electronic packaging technology,[16] which is shrinking in size to the nanoscale. Most of these applications use dielectric properties below the gigahertz (GHz) frequency range and therefore impedance spectroscopy (IS) is used to determine the electrical capacitance of the material in parallel-plate capacitor or the dielectric constant of the material under investigation. The capacitor equation is also frequently used in the characterization of field effect transistors for determining parameters such as charge-carrier mobilities[17−20] and transconductance.[18,21,22] In Mott−Schottky analysis, the flat-capacitor equation is implicitly applied to determine the doping density of semiconductors, the width of the depletion region, and the flat-band potential of the semiconductor/metal interfaces.[23,24]

Considering its broad application, the accuracy of the capacitor equation is very important, especially for finding credible routes to design novel materials for nanoelectronics. The accuracy of the equation is often considered to be associated with the uncertainty of the contributing parameters in the equation.[25] Among these parameters, the reliability of the capacitance has been addressed the most by introducing experimental strategies for performing the capacitance measurements correctly.[25−28] However, the precision of the individual parameters of the equation does not guarantee the accuracy of the relation between them, in case the assumptions made in deriving the relation itself are not completely met. One of these assumptions is that the parallel-plate capacitor electrodes are ideally smooth and flat. In a simplistic picture, the degree of the smoothness of a surface depends on the distance at which the surface is observed. An electrode with micro- or nanoscale roughness can be considered smooth for a capacitor with macroscale thickness, whereas for a thin-film capacitor, the assumption of a flat and smooth electrode is violated.

Received: May 10, 2017
Accepted: July 26, 2017
Published: July 26, 2017

DOI: 10.1021/acsami.7b06451
ACS Appl. Mater. Interfaces 2017, 9, 27290−27297

In a theoretical study, Zhao et al. have discussed the interface roughness effect on the electric field, the capacitance, and the leakage current of an insulating film in a parallel-plate capacitor.[29] In this work, and several following theoretical and computational studies, the capacitance was shown to be electronically coupled to the roughness characteristics of the electrodes.[30−34] Even though the presence of surface roughness is very common for solid-state thin films, apart from a few studies on specific systems, no general experimental work on the influence of the realistic roughness of the electrodes on the electrical capacitance of thin-film capacitors has been reported.[35−37] This means that the impact of the interface roughness on the electrical capacitance of thin films has been grossly overlooked within the nanoelectronic community.

In this study, we experimentally demonstrate that thin-film capacitors with a rough electrode show a higher electrical capacitance than the value predicted from the parallel-plate capacitor formula. Some of the capacitors show deviations of up to 50% among the investigated capacitors, including amorphous dielectric polymer thin films and small-molecule semiconductors. To study the connection between the interface roughness and the electrical capacitance enhancement, we exploit the extended parallel-plate capacitance formula derived by Zhao et al.[29] In this formula, the excess capacitance originated from the weak roughness of an electrode is calculated by incorporating the roughness parameters. Experimentally, we determine the roughness parameters by analyzing the topography images of the rough electrode obtained by atomic force microscopy (AFM). Independently, we determine the electrical capacitance of the capacitors using impedance spectroscopy. The observed correlation between the capacitance values and roughness characteristics of the electrodes agrees with the predictions of the extended parallel-plate capacitor formula.

2. THEORY

The capacitance of an empty parallel-plate capacitor is calculated from the well-known textbook formula

$$C_0 = \varepsilon_0 \frac{A}{h_0} \tag{1}$$

where ε_0 is the electric permittivity of vacuum, h_0 is the distance between the plates, and A is the area of the plates. This formula is derived from Gauss's law with two important assumptions: (1) the area of the plates is infinitely large compared to the distance between the plates and (2) the plates are flat and smooth. If a dielectric material fills the space between the metal plates, the capacitance increases by a factor of ε_r called the relative dielectric constant or the relative static permittivity.

$$\frac{C_f}{C_0} = \varepsilon_r \tag{2}$$

where C_f denotes the capacitance of the capacitor with ideally flat and smooth electrodes. The dielectric constant of a material generally depends on the chemical structure, defects, temperature, pressure, and the frequency of the applied alternating field. As long as these factors remain identical for the filler, it can be seen from eq 2 that the dielectric constant of the filler and the geometrical dimensions of the capacitor are the only factors playing a role in the electrical capacitance of the capacitor with two smooth plates. In practice, thin-film capacitors meet the first assumption for the parallel-plate capacitor formula because the thickness of the films is usually orders of magnitude smaller than the lateral dimensions of the plates. However, the second assumption may not be met for some thin-film capacitors due to the roughness of the interface (see Figure 1). It is necessary to reformulate the capacitance equation for thin-film capacitors with rough interfaces.

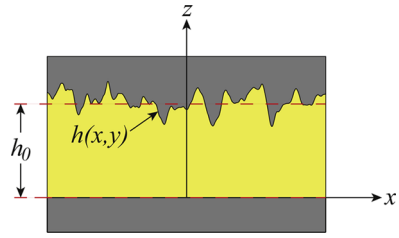

Figure 1. Schematic cross section of the capacitors with one rough contact. The dashed line shows the average thickness of the film, h_0.

To determine the electrical contribution of a rough electrode to the total capacitance of a capacitor, we must first characterize the roughness. Similar to most surfaces found in nature, the topology of a wide variety of thin films is well described by self-affine roughness, regardless of their growth technique. In self-affine roughness, fractal remains statistically similar but is scaled differently in different directions.[38−40] Three characteristic parameters are defined to describe a self-affine rough surface: (1) the *root-mean-square* (rms) roughness, σ, which is the root-mean-square average of the profile height deviations from the mean height; (2) the *lateral correlation length*, ξ, which is an upper in-plane scaling cutoff indicating the length at which a point on the surface follows the memory of its initial value upon moving on the surface; and (3) the *roughness exponent*, α, which defines the irregularity of the surface and has a value between 0 and 1. Small values of α ($\approx$0) represent extremely jagged surfaces, whereas larger values ($\approx$1) represent smooth hills and valleys.

The roughness parameters can be determined by correlation functions of the surface. The height difference (or height−height) correlation function (HHCF) is defined as $H(\mathbf{r}) = \langle[z(\mathbf{r}) - z(\mathbf{r}_0)]^2\rangle$, where $\mathbf{r}$ is the in-plane positional vector, $z(\mathbf{r})$ is the surface height, and $\langle\rangle$ is indicative of a spatial average over the planar reference surface. For the self-affine roughness, the HHCF follows the scaling behavior given by

$$H(r) \propto r^{2\alpha}, \quad r \ll \xi \tag{3a}$$

$$H(r) = 2\sigma^2, \quad r \gg \xi \tag{3b}$$

These parameters are required to describe the roughness of the electrode.

To derive the roughness-dependent capacitance formula, Palasantzas and co-workers followed an analytic approach[29,30] that we briefly summarize here. In this approach, the Laplace equation ($\nabla^2\Phi(x, y, z) = 0$) is solved for a capacitor with one rough and one smooth electrode to determine the electrostatic potential between the plates (see Figure 1). $\Phi(x, y, z = 0) = 0$ for the smooth plate and $\Phi(x, y, z = h_0 + h(x, y)) = V$ for the rough plate with surface height fluctuations of $h(x, y)$ were used as the boundary conditions. The perturbation method is applied for the potential on the rough boundary to solve the Laplace equation. Because a weak roughness is assumed, perturbation orders greater than 2 are dropped from the calculations. For a weak roughness, the rms local surface slope is small ($\sqrt{\langle|\nabla h|^2\rangle} \ll 1$).[29,30] The remaining terms depend on

DOI: 10.1021/acsami.7b06451
ACS Appl. Mater. Interfaces 2017, 9, 27290−27297

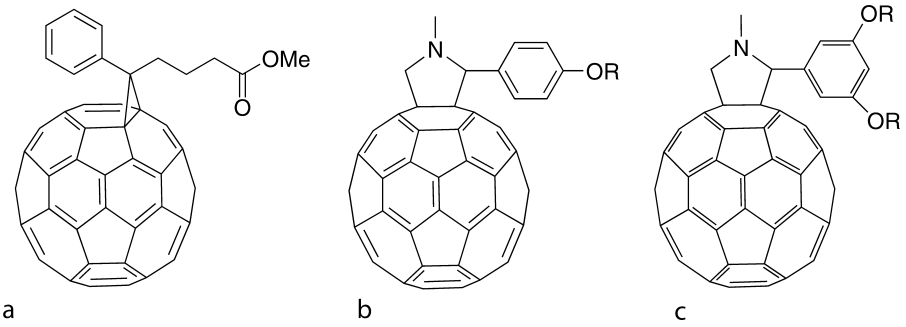

Figure 2. Chemical structures of fullerene derivatives: (a) [60]PCBM, (b) PDEG-1 (R═$(CH_2CH_2O)_2CH_3$), PTeEG-1 (R═$(CH_2CH_2O)_4CH_2CH_3$), and (c) PTeEG-2 (R═$(CH_2CH_2O)_4CH_2CH_3$).

the height fluctuations and are replaced by the roughness spectrum derived for self-affine fractal scaling. The electrostatic potential of the rough electrode is then derived depending on the roughness parameters. The electric field within the capacitor is calculated from the electrostatic potential difference between the plates. Ultimately, an extended parallel-plate capacitor equation is derived, which includes the excess capacitance of the rough electrode

$$C_{r/f} \equiv \frac{C_r}{C_f} = 1 + f(\sigma, \alpha, \xi) \tag{4}$$

where C_r is the capacitance of a capacitor with one rough electrode and $f(\sigma, \alpha, \xi)$ follows

$$f(\sigma, \alpha, \xi) \equiv f_{r1} + f_{r2} \approx \frac{\sigma^2}{a\xi^2}\left\{\frac{(1 + ak_c^2\xi^2)^{1-\alpha} - 1}{1 - \alpha} - 2a\right\} + \frac{1}{h_0}\int_0^{k_c} \frac{\cosh(kh_0)}{\sinh(kh_0)} k^2 \frac{\sigma^2\xi^2}{(1 + ak^2\xi^2)^{1+\alpha}}\, dk \tag{5}$$

where $k_c = \pi/a_c$ is the upper cutoff of the spatial frequency, with a_c as the size of the smallest feature of the surface, and a is a normalization parameter calculated from

$$a = (1/2\alpha)[1 - (1 + ak_c^2\xi^2)^{-\alpha}] \tag{6}$$

The f_{r1} and f_{r2} coefficients determine the contribution of increased effective area and enhanced electric field to the capacitance, respectively. In other words, the effective area of a rough electrode is larger than that of a flat and smooth electrode; therefore, more charge can be stored on the electrode, leading to an increased capacitance. Furthermore, the electric field is enhanced at the sharp hills and valleys of the rough interface, leading to charge accumulation at these spots and thereby enhanced electrical capacitance.

The knowledge of the $C_{r/f}$ value allows us to correct the overestimated dielectric constant of the filler material after the capacitance measurement of a capacitor with a rough electrode. Conversely, the knowledge of the roughness parameters of the interface allows us to predict the electrical capacitance of a rough capacitor without underestimating it by using eq 2.

It is important to note that in the derivation of eq 5, a simple Lorentzian model[40] is used to describe the roughness spectrum. Other roughness models may lead to a different formulation, yet the fact that the interface roughness gives rise to a capacitance in excess of that found for the case of a flat capacitor remains unchanged. Therefore, it is not generally applicable for all topologies. Moreover, knowledge of the lower cutoff size of the topology, a_c, is essential for correctly estimating the value of the excess capacitance. In this work, we use eq 5 as a guide to understand the link between the interface roughness and the enhanced capacitance upon roughening the interface.

3. RESULTS AND DISCUSSION

To experimentally investigate the excess capacitance of a rough electrode, we fabricate parallel-plate capacitors with one smooth and one rough electrode. For the smooth electrode, we use indium tin oxide (ITO) covered with poly(3,4-ethylenedioxythiophene):polystyrene sulfonate (PEDOT:PSS). Compared to a metallic electrode, ITO provides better wetting for the solution-processed compounds and is more stable toward the common solution-processing solvents. Because the coarse surface of ITO is not ideal for our study, we cover it with PEDOT:PSS to form a smooth interface at the bottom electrode (see Figure S1). To vary the roughness at the interface of the metallic top electrode (Al here), we change the surface roughness of the filler so that the top contact replicates the topology upon evaporation (Figure 1). Processing fillers from solvents with different volatility allows us to tailor the surface roughness of the filler. Provided that the dielectric properties of the bulk remain unchanged, we are able to compare the roughness dependence of the capacitance exclusively. Solution-processable amorphous compounds are most suited for this purpose because we can alter the surface topology by changing the processing conditions yet yield films that share the same dielectric properties due to their amorphous nature. We determine the capacitance of the capacitors using impedance measurements (referred as C_m throughout the text). A deviation of C_m/C_0 from ε_r, the intrinsic dielectric constant of the filler material, then serves as an indication of the excess capacitance due to the rough electrode (see eqs 2 and 4). The strategies applied in this work to accurately determine C_m and C_0 are described in the Supporting Information.

3.1. Smooth Capacitors. To distinguish between the deviations arising from the roughness effect and the deviations due to measurement errors, we first estimate the overall error of the dielectric constant determined from the ideally smooth parallel-plate capacitors. The chemical structure of [6,6]-phenyl C_{61} butyric acid methyl ester ([60]PCBM) is shown in Figure 2a. It is known that as-spun films of [60]PCBM are amorphous.[41,42] Therefore, it is possible to process PCBM from different solvents to obtain different film thicknesses and morphologies while not altering its intrinsic dielectric constant.

DOI: 10.1021/acsami.7b06451
ACS Appl. Mater. Interfaces 2017, 9, 27290−27297

We fabricated several [60]PCBM capacitors by spin coating from orthodichlorobenzene (ODCB), chloroform ($CHCl_3$), and chlorobenzene. Because all of the processed films had smooth surfaces ($\sigma < 1$ nm), we could use eq 2 to determine ε_r. Figure 3 shows the values of ε_r for 44 capacitors in 11 different

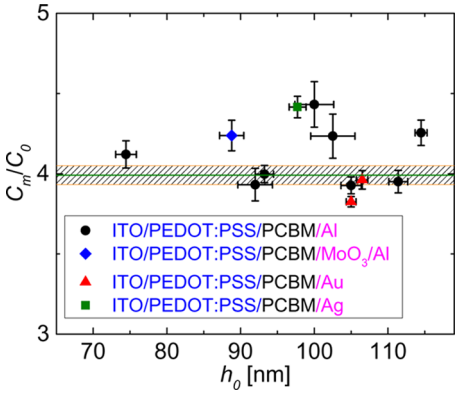

Figure 3. C_m/C_0 vs average film thickness for [60]PCBM using different contacts. For capacitors with Al top contact, [60]PCBM is processed from $CHCl_3$, chlorobenzene, and ODCB. For the remaining capacitors, it is processed from $CHCl_3$. Different processing conditions (spinning speed and open- or closed-cap spin coating) are applied for the films. The green line is the weighted mean of C_m/C_0, and the dashed area shows the standard error of the mean.

film thicknesses with the weighted average of $\overline{\varepsilon_r} = 4.0 \pm 0.1$. This means that, by using an adequate number of measurements, we can minimize the standard error of the mean to $\Delta\varepsilon = \pm 0.1$ or the relative error to 3% for ε_r. We tested the dielectric constant of thermally evaporated C_{60} thin films in the ITO/PEDOT:PSS/C_{60}/Al capacitor structure. All of the C_{60} films showed a smooth surface enabling the reliable determination of ε_r values from eq 2. We found no difference that can be resolved beyond the error margin between ε_r of [60]PCBM and C_{60}. Therefore, vis-à-vis the dielectric constant, the bulk of these fullerene derivatives do not go through a major change when ordinary growth methods are used.

3.2. Rough Capacitors: Determining Excess Capacitance. By investigating the capacitance of fullerene derivatives with ethyleneoxy side chains shown in Figure 2b,c, we obtained scattered values of C_m/C_0 for different processing conditions (reported in Table S1). It is unlikely that the intrinsic dielectric constant of the tested fullerene derivatives undergoes a significant change through the variation of simple processing conditions. Therefore, the variations of C_m/C_0 are more likely to originate from the interface effect on the electrical capacitance.

Figure 4 shows sample AFM images of smooth and rough surfaces of PDEG-1, and Figure 5 reports all C_m/C_0 values of

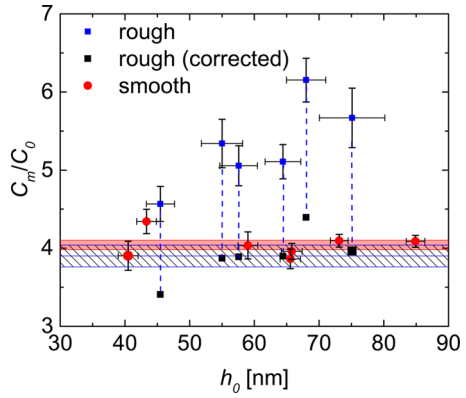

Figure 5. C_m/C_0 vs average film thickness for PDEG-1. The red symbols indicate the results obtained from smooth samples, and the red filled line shows $\overline{\varepsilon_r} = \overline{C_m/C_0} = 4.1 \pm 0.1$. The blue symbols attached with dashed lines (guide to the eye) to the black symbols indicate the results from rough samples before and after the elimination of the excess capacitance. The blue line with the dashed area shows $\overline{C_m/C_0} = 3.9 \pm 0.2$ from rough samples after elimination of the interface capacitance.

PDEG-1 processed into smooth and rough films, where the red symbols represent the values obtained from the smooth samples so that we find the dielectric constant of PDEG-1 as $\overline{\varepsilon_r} = \overline{C_m/C_0} = 4.1 \pm 0.1$, and the blue symbols show the C_m/C_0 values obtained from the rough films that are significantly larger than those of the smooth films. It is clear that additional capacitance is created by the interface roughness at the top electrode. The additional capacitance cannot be resolved from impedance data because it creates an additional capacitance in parallel with the bulk (see Figures S2 and S3).

To correct the C_m/C_0 values obtained from rough capacitors for the excess capacitance, we performed the following procedure: we analyzed the topography of rough interfaces acquired by AFM to plot HHCF. Using eqs 3a and 3b, we extracted σ, α, and ξ from the HHCF plot, as indicated in Figure 6. By plugging the obtained roughness parameters into eq 5 and assuming $a_c = 1$ nm, approximately equal to the size of the C_{60} molecule,[43] we calculated $f(\sigma, \alpha, \xi)$. Finally, we divided C_m/C_0 to $C_{r/f}$ from eq 4 to eliminate the excess capacitance of the rough interface from the total capacitance. The black

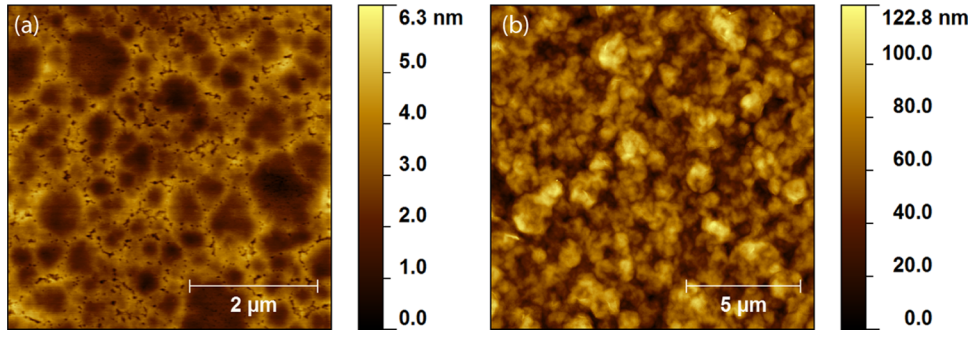

Figure 4. AFM images of (a) smooth and (b) rough interfaces of PDEG-1 capacitors.

DOI: 10.1021/acsami.7b06451
ACS Appl. Mater. Interfaces 2017, 9, 27290−27297

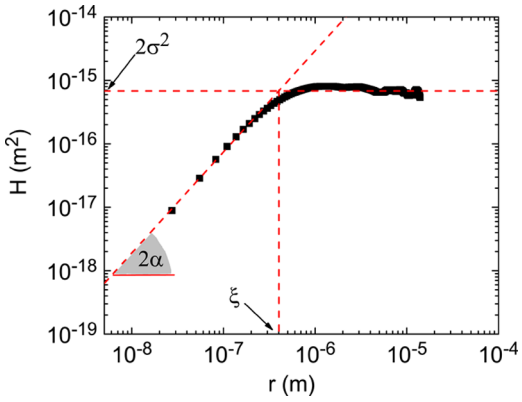

Figure 6. Height difference correlation function along fast scanning direction of the rough topography shown in Figure 4. All of the roughness parameters can be determined from this function.

symbols in Figure 5 show the corrected C_m/C_0 values, which in average give $\overline{C_m/C_0} \approx 3.9 \pm 0.2$, close to the intrinsic dielectric constant of PDEG-1. This means that the extended capacitance formula decouples the capacitance of the rough interface from the total electrical capacitance with good approximation.

We could not obtain accurate dielectric constant values for the two other fullerene derivatives, PTeEG-1 and PTeEG-2, because we could not fabricate the ideally smooth films. As listed in Table S1, the rough films showed roughness-dependent capacitance, for which we use the extended capacitance formula to eliminate the excess capacitance factor from the results. After the elimination, the resulting values show smaller standard deviation from the mean than the raw values. This proves that the variations of C_m/C_0 originate from the interface roughness of the PTeEG-1 and PTeEG-2 capacitors.

3.3. Rough Capacitors: Polymers. For polymers, it is difficult to define a specific atomic or molecular scale as the lower cutoff length of the topology because of the complex conformations of the chains close to the surface of the films. Therefore, calculation of the excess capacitance using eq 5 becomes problematic for a rough electrode formed at the interface with a polymer. For instance, we processed poly(vinyledene difluoride)-trifluoroethylene P(VDF-TrFE), with the molar ratio of 70/30 into both smooth and rough films. We did not apply a DC bias to the capacitors to not turn on the ferroelectric property of the copolymer.[44,45] All of the C_m/C_0 values converged to ≈11 for smooth and rough capacitors. Compared to the rough films of the fullerene derivatives, the roughness values of the P(VDF-TrFE) films were not negligible (see Table S1). However, it appears that, unlike the case of the fullerene derivatives, the interface roughness does not influence the capacitance of the P(VDF-TrFE) capacitors. We can speculate that the smooth P(VDF-TrFE) films have a different morphology than the rough films, leading to a greater bulk dielectric constant. However, it is known that the transition of P(VDF-TrFE) to a semicrystalline phase with enhanced dielectric constant does not occur without thermal annealing.[46,47] Because we measured all of the capacitors with as-cast P(VDF-TrFE) films, we do not expect that a different dielectric constant of the bulk for the smooth and rough films leads to identical C_m/C_0 values for all cases. Alternatively, it is possible that the cutoff length for the rough P(VDF-TrFE) surfaces is larger than that of the tested fullerene derivatives. By setting a_c > 70 nm, we obtain negligible $C_{r/f}$ for all of the rough capacitors

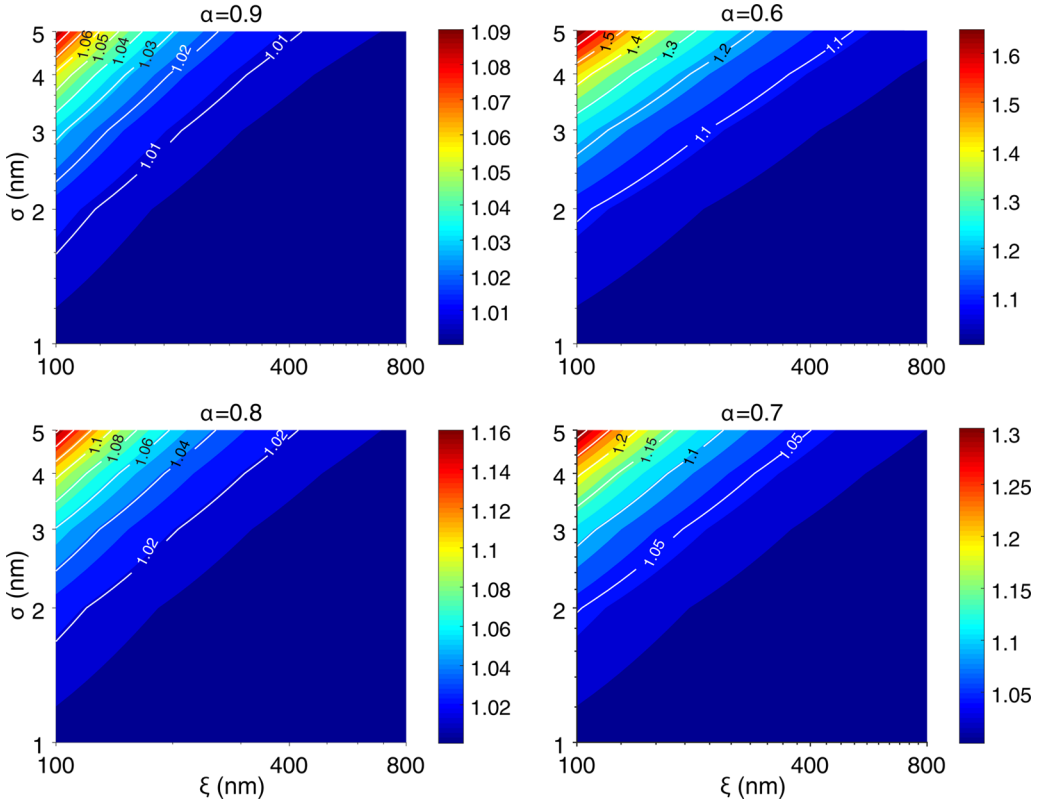

Figure 7. Contour plots of $C_{r/f}$ vs σ and ξ for various roughness exponents. The cutoff length is set to 1 nm, and the weak roughness limits are set to σ/ξ < 5% and σ/h_0 < 10% for all graphs. The average thickness of the rough films is assumed to be h_0 = 100 nm.

DOI: 10.1021/acsami.7b06451
ACS Appl. Mater. Interfaces 2017, 9, 27290−27297

(presented in Table S1), justifying the similar C_m/C_0 values for the rough and smooth films. Unfortunately, it is not possible to obtain the real value of a_c from the AFM images of the topology. Moreover, the link between the cutoff length of a surface and the bulk properties is a subject of an ongoing theoretical study. Therefore, we can only speculatively evaluate the appropriate value for a_c by estimating the lattice spacing or molecule size in a film, which is difficult to assign for polymers due to their complex morphology.

3.4. Dependence of Excess Capacitance on the Roughness Parameters. On the basis of these observations, we conclude that a_c and the three major roughness parameters (α, σ, and ξ) collectively contribute to the generation of the excess capacitance at the rough electrode. Therefore, it is worthwhile to study the contribution of different roughness parameters to the formation of excess capacitance in more detail. We define different roughness parameters for an electrode and calculate $C_{r/f}$ for the generated roughness using eq 5. As shown in Figure 7, $C_{r/f}$ increases by increasing the rms roughness and the lateral correlation length. The increase is sharper for less regular surfaces (smaller α). For instance, σ = 10 nm can be considered a large rms roughness for a capacitor with average film thickness of 100 nm. However, with the roughness exponent of 0.8, as long as the lateral correlation length is greater than 700 nm, a negligible excess capacitance is created by the rough electrode. On the contrary, σ = 2 nm cannot be neglected for an interface with a lateral correlation length smaller than 200 nm and the roughness exponent of 0.7. For identical roughness parameters, the excess capacitance of the surface with a smaller cutoff length is stronger (not shown in Figure 7). As can be seen in Table S1, f_{r1} values are greater than those of f_{r2}, which means that increased effective area due to roughness of the electrode plays a dominant role in the excess capacitance value.

3.5. Parameters Derived from Capacitor Equation. It is important to know the roughness limit at which the excess capacitance of the rough interface becomes negligible. If $C_{r/f}$ = 1.04 is considered as the tolerance limit for roughness effect, then σ/ξ should remain roughly below 0.01 for surfaces, with the roughness exponent of 0.6−0.7, whereas this limit is twice as large for more regular surfaces, with the roughness exponent of 0.8−0.9 (assuming a_c = 1 nm). In general, the rms roughness of ≈1 nm is small enough for most surfaces so that the interface roughness effect can be neglected for thin-film capacitors with h_0 > 50 nm. The defined limits may vary on the basis of the expected accuracy of the parameters extracted from the parallel-plate capacitor equation. For instance, in the determination of the dielectric constant from the capacitor equation, the roughness effect of the electrode cannot be resolved for $C_{r/f}$ up to 1.11 as long as a 10% relative error for ε_r is tolerated, whereas $C_{r/f}$ should remain below 1.02 to maintain the relative error of ε_r below 2%.

Considering that the dielectric constant is one of the most important parameters that is usually extracted from the parallel-plate capacitor equation, it is fruitful to propose a general protocol for the reliable determination of ε_r of a material. The most straightforward approach is to produce smooth capacitors of the material to ensure that the capacitor equation is applicable with dependable accuracy. By reproducing the results from several capacitors with smooth electrodes, the precision of ε_r is guaranteed along with its accuracy. Under the discussed conditions, ε_r can be reported with the accuracy of one decimal place, and considering the precision limits and the accuracy of the applied technique, two decimal places would be meaningless. For the capacitors with rough interfaces, reproducing the results may make the average outcome precise but not accurate. This is because we may produce identical roughness by repeating the same growth method for the films and repeatedly overestimate ε_r (see Table S1, PTeEG-1 processed from $CHCl_3$). The best approach is to smooth the interfaces prior to capacitance measurement by finding the correct deposition routes. If smoothing the interfaces is not possible, yet C_m/C_0 obtained from rough capacitors does not show any dependence on the changes of the interface roughness, as we observed for P(VDF-TrFE) copolymer, then the roughness effect can be ignored. When C_m/C_0 changes with the variations of the interface roughness, the roughness effect should not be neglected, otherwise the extracted ε_r from the simple parallel-plate capacitor equation will be overestimated. Similarly, the contribution of the film growth technique, bulk morphology, or the film crystalline structure to the bulk dielectric constant will be misinterpreted by ignoring the interface roughness effect.

In addition to the dielectric constant, there are other parameters that are determined using the parallel-plate capacitor equation, for which the reliability depends on the accuracy of the equation. If the roughness of the gate/dielectric interface is neglected in field effect transistors, then the capacitance of the gate dielectric can be underestimated, leading to the erroneous determination of the charge-carrier mobility in the conductive channel. Therefore, it is advisable to use the direct measurement of the gate capacitance instead of estimating it from the parallel-plate capacitor equation, in case a rough gate/dielectric interface is present in the transistor structure.

It is practically impossible to avoid the influence of the roughness on the capacitance for all thin-film capacitors. The extended parallel-plate capacitor equation presented in this work can calculate the excess capacitance of the rough interface commonly occurring for a wide range of thin-film capacitors. We have provided an in-house software interface available at http://www.photophysics-optoelectronics.nl/wp-content/uploads/2017/05/finalized-interface.7z to make the calculation of eq 5 convenient with given roughness parameters.

4. CONCLUSIONS

We experimentally showed that the realistic interface roughness of an electrode can give rise to an enhanced electrical capacitance in thin-film capacitors. Using an extended parallel-plate capacitor equation, in which the roughness of the electrode is considered via a theoretical model, we were able to explain our experimental observations in terms of the roughness parameters. Using the presented model, we found that the excess capacitance of the rough electrode not only depends on the rms roughness (which is the most commonly cited roughness parameter) but also on the lateral correlation length and the roughness exponent. The roughness model used for the thin films in this study is applicable to the roughness normally occurring in labs with common film-deposition techniques. Nevertheless, the formulated extended parallel-plate capacitor equation is applicable only to the capacitors with one rough electrode. Further study is required to obtain a complete picture that includes both rough electrodes. Considering the adverse impacts of unreliable information obtained from the parallel-plate capacitor method with inadequate accuracy, such study is highly necessary.

DOI: 10.1021/acsami.7b06451
ACS Appl. Mater. Interfaces 2017, 9, 27290−27297

5. EXPERIMENTAL SECTION

5.1. Materials. PEDOT:PSS water dispersion (Clevios VP AI 4083) was acquired from Heraeus. [60]PCBM and C_{60} were purchased from Solenne Co. The synthesis details of PDEG-1, PTeEG-1, and PTeEG-2 will be reported elsewhere.

5.2. Preparation of Capacitors. Commercially available indium tin oxide (ITO)-patterned glass substrates with different dimensions (9, 16, 36, and 100 mm^2) were used as the bottom electrode for all capacitors. The ITO substrates were cleaned by being scrubbed with soapy water solution, flushed with deionized water, separately sonicated in acetone and isopropyl alcohol, and then oven-dried and subjected to a UV-ozone treatment. PEDOT:PSS was filtered through TPFE filters (0.45 μm) and spin-cast under ambient condition and dried at 140 °C for 10 min. The filler materials were solution-processed except C_{60}, which was thermally evaporated. Aluminum top contacts with a thickness of 100 nm were deposited by a thermal evaporation process at a pressure less than 10^{-7} mbar.

5.3. Characterizations. Impedance spectroscopy was performed with a Solartron 1260 impedance gain-phase analyzer with gold-plated spring probes from Feinmetall GMBH. AFM topographical images were recorded in tapping mode using a Bruker MultiMode AFM-2 with TESP probes. All of the sample-processing steps and measurements were carried out under an N_2 atmosphere at a stable temperature, except for the AFM measurements, which were performed under ambient conditions.

■ ASSOCIATED CONTENT

Supporting Information

The Supporting Information is available free of charge on the ACS Publications website at DOI: 10.1021/acsami.7b06451.

AFM images of ITO and PEDOT:PSS; determining C_m with impedance spectroscopy; determining C_0; determining the roughness parameters; film specifications and roughness parameters of PDEG-1, PTeEG-2, PTeEG-1, and PVDF-TrFE; and the corresponding values of C_m/C_0 before and after eliminating the excess capacitance of the rough electrode (PDF)

■ AUTHOR INFORMATION

Corresponding Author

*E-mail: s.torabi@rug.nl. Phone: +31 (0)50 3635211.

ORCID

Solmaz Torabi: 0000-0003-1612-3518

L. Jan Anton Koster: 0000-0002-6558-5295

Notes

The authors declare no competing financial interest.

■ ACKNOWLEDGMENTS

The authors would like to thank S. Solhjoo for discussions of roughness analysis and J. Xu for technical guidance on polymer processing. S.T. and L.J.A.K. thank J. Zaumseil for useful discussions on transistors. This work was supported by Foundation for Fundamental Research on Matter (FOM), which is part of the Netherlands Organisation for Scientific Research (NWO), by grant FOM-G-23. This is a publication by the FOM Focus Group *Next Generation Organic Photovoltaics*, participating in the Dutch Institute for Fundamental Energy Research (DIFFER).

■ REFERENCES

(1) Kingon, A. I.; Maria, J.-P.; Streiffer, S. Alternative Dielectrics to Silicon Dioxide for Memory and Logic Devices. *Nature* **2000**, *406*, 1032−1038.

(2) Cava, R.; Peck, W., Jr.; Krajewski, J. Enhancement of the Dielectric Constant of Ta_2O_5 Through Substitution with TiO_2. *Nature* **1995**, *377*, 215.

(3) Chen, Q.; Shen, Y.; Zhang, S.; Zhang, Q. Polymer-Based Dielectrics with High Energy Storage Density. *Annu. Rev. Mater. Res.* **2015**, *45*, 433−458.

(4) Chen, Q.; Wang, Y.; Zhou, X.; Zhang, Q.; Zhang, S. High Field Tunneling as a Limiting Factor of Maximum Energy Density in Dielectric Energy Storage Capacitors. *Appl. Phys. Lett.* **2008**, *92*, No. 142909.

(5) Rao, Y.; Ogitani, S.; Kohl, P.; Wong, C. Novel Polymer−Ceramic Nanocomposite Based on High Dielectric Constant Epoxy Formula for Embedded Capacitor Application. *J. Appl. Polym. Sci.* **2002**, *83*, 1084−1090.

(6) Lu, J.; Moon, K.-S.; Xu, J.; Wong, C. Synthesis and Dielectric Properties of Novel High-K Polymer Composites Containing In-Situ Formed Silver Nanoparticles for Embedded Capacitor Applications. *J. Mater. Chem.* **2006**, *16*, 1543−1548.

(7) Chen, Y.; Xia, Y.; Sun, H.; Smith, G. M.; Yang, D.; Ma, D.; Carroll, D. L. Solution-Processed Highly Efficient Alternating Current-Driven Field-Induced Polymer Electroluminescent Devices Employing High-K Relaxor Ferroelectric Polymer Dielectric. *Adv. Funct. Mater.* **2014**, *24*, 1501−1508.

(8) Koster, L.; Shaheen, S. E.; Hummelen, J. C. Pathways to a New Efficiency Regime for Organic Solar Cells. *Adv. Energy Mater.* **2012**, *2*, 1246−1253.

(9) Torabi, S.; Jahani, F.; Van Severen, I.; Kanimozhi, C.; Patil, S.; Havenith, R. W. A.; Chiechi, R. C.; Lutsen, L.; Vanderzande, D. J. M.; Cleij, T. J.; Hummelen, J. C.; Koster, L. J. A. Title Case Strategy for Enhancing the Dielectric Constant of Organic Semiconductors Without Sacrificing Charge Carrier Mobility and Solubility. *Adv. Funct. Mater.* **2015**, *25*, 150−157.

(10) Brochu, P.; Pei, Q. Advances in Dielectric Elastomers for Actuators and Artificial Muscles. *Macromol. Rapid Commun.* **2010**, *31*, 10−36.

(11) Anderson, I. A.; Gisby, T. A.; McKay, T. G.; O Brien, B. M.; Calius, E. P. Multi-Functional Dielectric Elastomer Artificial Muscles for Soft and Smart Machines. *J. Appl. Phys.* **2012**, *112*, No. 041101.

(12) Zhang, Q. M.; Li, H.; Poh, M.; Xia, F.; Cheng, Z.-Y.; Xu, H.; Huang, C. An All-Organic Composite Actuator Material with a High Dielectric Constant. *Nature* **2002**, *419*, 284−287.

(13) Kharroub, S.; Laflamme, S.; Song, C.; Qiao, D.; Phares, B.; Li, J. Smart Sensing Skin for Detection and Localization of Fatigue Cracks. *Smart Mater. Struct.* **2015**, *24*, No. 065004.

(14) Jia, Y.; Sun, K.; Agosto, F. J.; Quinones, M. T. Design and Characterization of a Passive Wireless Strain Sensor. *Meas. Sci. Technol.* **2006**, *17*, 2869.

(15) Zirkl, M.; Haase, A.; Fian, A.; Schön, H.; Sommer, C.; Jakopic, G.; Leising, G.; Stadlober, B.; Graz, I.; Gaar, N.; Schwödiauer, R.; Bauer-Gogonea, S.; Bauer, S. Low-Voltage Organic Thin-Film Transistors with High-K Nanocomposite Gate Dielectrics for Flexible Electronics and Optothermal Sensors. *Adv. Mater.* **2007**, *19*, 2241−2245.

(16) Pushkar, J.; Rymaszewski, E. J. *Thin-Film Capacitors for Packaged Electronics*; Springer Science & Business Media, 2003.

(17) Bisri, S. Z.; Gao, J.; Derenskyi, V.; Gomulya, W.; Iezhokin, I.; Gordiichuk, P.; Herrmann, A.; Loi, M. A. High Performance Ambipolar Field-Effect Transistor of Random Network Carbon Nanotubes. *Adv. Mater.* **2012**, *24*, 6147−6152.

(18) Wunnicke, O. Gate Capacitance of Back-Gated Nanowire Field-Effect Transistors. *Appl. Phys. Lett.* **2006**, *89*, No. 083102.

(19) Chen, F.-C.; Chu, C.-W.; He, J.; Yang, Y.; Lin, J.-L. Organic Thin-Film Transistors with Nanocomposite Dielectric Gate Insulator. *Appl. Phys. Lett.* **2004**, *85*, 3295−3297.

(20) Stadlober, B.; Zirkl, M.; Beutl, M.; Leising, G.; Bauer-Gogonea, S.; Bauer, S. High-Mobility Pentacene Organic Field-Effect Transistors with a High-Dielectric-Constant Fluorinated Polymer Film Gate Dielectric. *Appl. Phys. Lett.* **2005**, *86*, No. 242902.

(21) Javey, A.; Kim, H.; Brink, M.; Wang, Q.; Ural, A.; Guo, J.; McIntyre, P.; McEuen, P.; Lundstrom, M.; Dai, H. High-κ Dielectrics for Advanced Carbon-Nanotube Transistors and Logic Gates. *Nat. Mater.* **2002**, *1*, 241−246.
(22) Duan, X.; Niu, C.; Sahi, V.; Chen, J.; Parce, J. W.; Empedocles, S.; Goldman, J. L. High-Performance Thin-Film Transistors Using Semiconductor Nanowires and Nanoribbons. *Nature* **2003**, *425*, 274−278.
(23) Nigam, A.; Premaratne, M.; Nair, P. R. On the Validity of Unintentional Doping Densities Extracted Using Mott−Schottky Analysis for Thin Film Organic Devices. *Org. Electron.* **2013**, *14*, 2902−2907.
(24) Kirchartz, T.; Gong, W.; Hawks, S. A.; Agostinelli, T.; MacKenzie, R. C.; Yang, Y.; Nelson, J. Sensitivity of the Mott−Schottky Analysis in Organic Solar Cells. *J. Phys. Chem. C* **2012**, *116*, 7672−7680.
(25) Andeen, C.; Fontanella, J.; Schuele, D. Accurate Determination of the Dielectric Constant by the Method of Substitution. *Rev. Sci. Instrum.* **1970**, *41*, 1573−1576.
(26) Barsoukov, E.; Macdonald, J. R. *Impedance Spectroscopy: Theory, Experiment, and Applications*; John Wiley & Sons, 2005.
(27) Cha, Y.; Aureli, M.; Porfiri, M. A Physics-Based Model of the Electrical Impedance of Ionic Polymer Metal Composites. *J. Appl. Phys.* **2012**, *111*, No. 124901.
(28) Martin, Y.; Abraham, D. W.; Wickramasinghe, H. K. High-Resolution Capacitance Measurement and Potentiometry by Force Microscopy. *Appl. Phys. Lett.* **1988**, *52*, 1103−1105.
(29) Zhao, Y.-P.; Wang, G.-C.; Lu, T.-M.; Palasantzas, G.; De Hosson, J. T. M. Surface-Roughness Effect on Capacitance and Leakage Current of an Insulating Film. *Phys. Rev. B* **1999**, *60*, 9157.
(30) Palasantzas, G. Self-Affine Roughness Influence on the Pull-in Voltage in Capacitive Electromechanical Devices. *J. Appl. Phys.* **2005**, *98*, No. 034505.
(31) Jamali, T.; Farahani, S. V.; Jannesar, M.; Palasantzas, G.; Jafari, G. Surface Coupling Effects on the Capacitance of Thin Insulating Films. *J. Appl. Phys.* **2015**, *117*, No. 175308.
(32) Palasantzas, G.; De Hosson, J. T. M. The Effect of Mound Roughness on the Electrical Capacitance of a Thin Insulating Film. *Solid State Commun.* **2001**, *118*, 203−206.
(33) Patrikar, R. M.; Dong, C. Y.; Zhuang, W. Modelling Interconnects with Surface Roughness. *Microelectron. J.* **2002**, *33*, 929−934.
(34) Zhu, Z.; White, J.; Demir, A. A Stochastic Integral Equation Method for Modeling the Rough Surface Effect on Interconnect Capacitance. *Proceedings of the 2004 IEEE/ACM International Conference on Computer-Aided Design*, 2004; pp 887−891.
(35) Aureli, M.; Lin, W.; Porfiri, M. On the Capacitance-Boost of Ionic Polymer Metal Composites Due to Electroless Plating: Theory and Experiments. *J. Appl. Phys.* **2009**, *105*, No. 104911.
(36) Albina, A.; Taberna, P.-L.; Cambronne, J.; Simon, P.; Flahaut, E.; Lebey, T. Impact of the Surface Roughness on the Electrical Capacitance. *Microelectron. J.* **2006**, *37*, 752−758.
(37) Son, J.; Maeng, W.; Kim, W.-H.; Shin, Y.; Kim, H. Interface Roughness Effect Between Gate Oxide and Metal Gate on Dielectric Property. *Thin Solid Films* **2009**, *517*, 3892−3895.
(38) Kulatilake, P.; Um, J. Requirements for Accurate Quantification of Self-affine Roughness Using the Roughness−length Method. *Int. J. Rock Mech. Min. Sci.* **1999**, *36*, 5−18.
(39) Meakin, P. The Growth of Rough Surfaces and Interfaces. *Phys. Rep.* **1993**, *235*, 189−289.
(40) Palasantzas, G. Roughness Spectrum and Surface Width of Self-Affine Fractal Surfaces via the K-Correlation Model. *Phys. Rev. B* **1993**, *48*, 14472.
(41) Yang, Y.; Liu, C.; Gao, S.; Li, Y.; Wang, X.; Wang, Y.; Minari, T.; Xu, Y.; Wang, P.; Zhao, Y. Large [6, 6]-phenyl C_{61} butyric acid methyl (PCBM) hexagonal Crystals Grown by Solvent-Vapor Annealing. *Mater. Chem. Phys.* **2014**, *145*, 327−333.
(42) Tregnago, G.; Wykes, M.; Paternó, G. M.; Beljonne, D.; Cacialli, F. Low-Temperature Photoluminescence Spectroscopy of Solvent-Free PCBM Single-Crystals. *J. Phys. Chem. C* **2015**, *119*, 11846−11851.
(43) Goel, A.; Howard, J. B.; Vander Sande, J. B. Size Analysis of Single Fullerene Molecules by Electron Microscopy. *Carbon* **2004**, *42*, 1907−1915.
(44) Lovinger, A. J. Ferroelectric Polymers. *Science* **1983**, *220*, 1115−1121.
(45) Zhang, Q. M.; Bharti, V.; Zhao, X. Giant Electrostriction and Relaxor Ferroelectric Behavior in Electron-Irradiated Poly (vinylidene fluoride-trifluoroethylene) Copolymer. *Science* **1998**, *280*, 2101−2104.
(46) Tajitsu, Y.; Ogura, H.; Chiba, A.; Furukawa, T. Investigation of Switching Characteristics of Vinylidene fluoride/trifluoroethylene Copolymers in Relation to Their Structures. *Jpn. J. Appl. Phys.* **1987**, *26*, 554.
(47) Benz, M.; Euler, W. B. Determination of the Crystalline Phases of Poly (vinylidene fluoride) Under Different Preparation Conditions Using Differential Scanning Calorimetry and Infrared Spectroscopy. *J. Appl. Polym. Sci.* **2003**, *89*, 1093−1100.

DOI: 10.1021/acsami.7b06451
ACS Appl. Mater. Interfaces 2017, 9, 27290−27297